University of Glasgow

DEPARTMENT OF

AEROSPACE ENGINEERING

The Helinv Numerical Algorithm

Dr Douglas G. Thomson

Internal Report No. 9408
June 1994

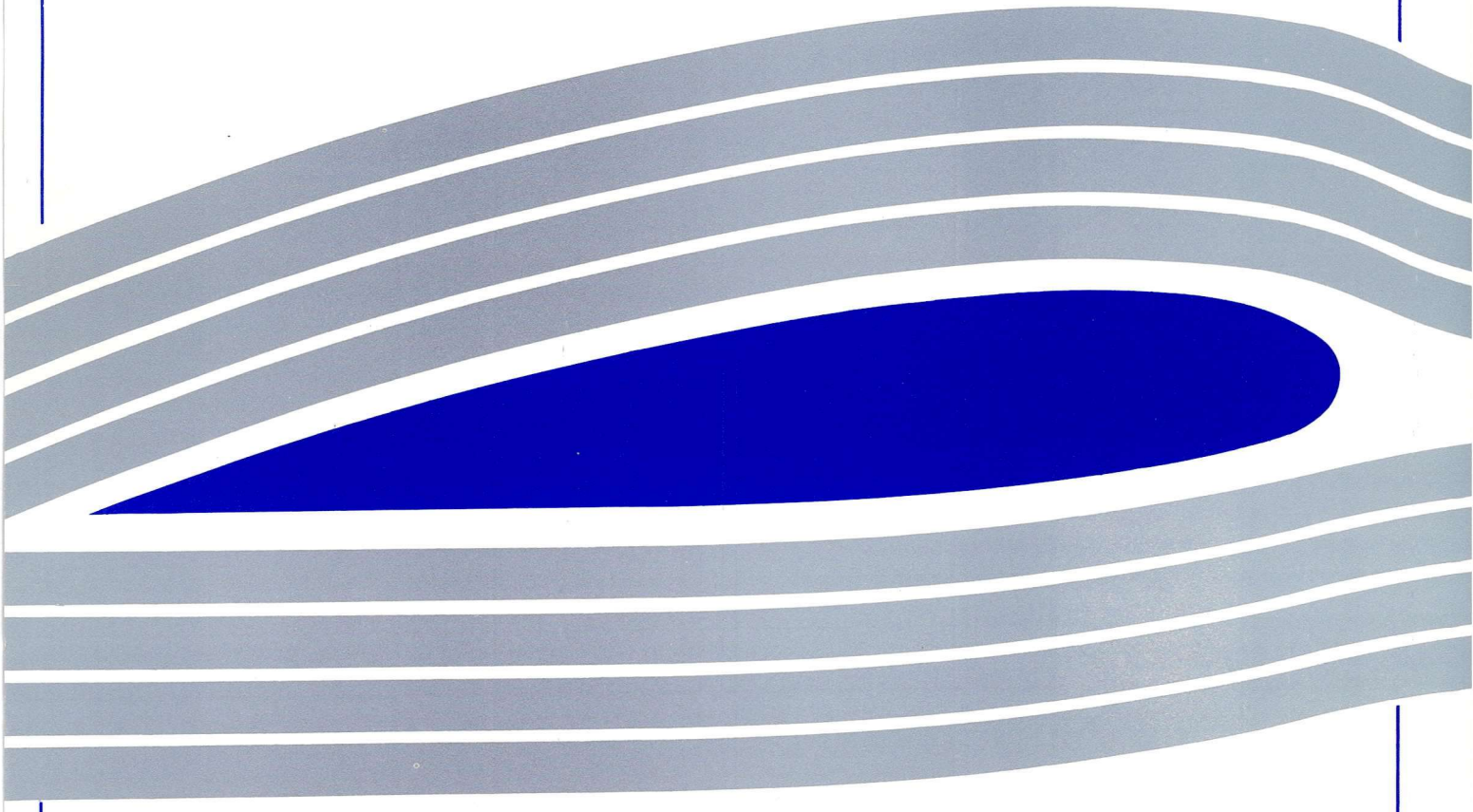

The Helinv Numerical Algorithm

Dr Douglas G. Thomson

Internal Report No. 9408
June 1994

Summary

This report gives a comprehensive description of the helicopter inverse simulation algorithm used in the latest generation of the package Helinv. As well as the description of the algorithm some results are presented, and a verification and validation of the algorithm is presented. Features unique to the results of inverse algorithms are also discussed along with the problems associated with the use of numerical differentiation, and finally an alternative scheme is outlined.

Contents

Nomenclature

g	acceleration due to gravity	(m/s^2)
h	height of obstacle in hurdle-hop manoeuvre	(m)
I_R	inertia of main rotor	$(kg\ m^2)$
I_{tr}	effective inertia of transmission and gearing	$(kg\ m^2)$
I_{xx}, I_{yy}, I_{zz}	helicopter moments of inertia about centre of gravity	$(kg\ m^2)$
I_{xz}	helicopter product of inertia about y-axis	$(kg\ m^2)$
K_3	overall gain of engine/rotorspeed governor	(Nm/rad/s)
$l_1, ..., n_3$	direction cosines for Euler transformation	
L, M, N	components of external moments on vehicle	(Nm)
m	helicopter mass	(kg)
p, q, r	components of helicopter angular velocity at centre of gravity	(rad/s)
Q_E	engine torque output	(Nm)
u, v, w	translational velocity components of helicopter centre of gravity	(m/s)
V_f	helicopter flight velocity	(m/s)
X, Y, Z	components of external force on vehicle	(N)

Greek Symbols

α	angle of incidence the fuselage	(rad)
β	main rotor blade flapping angle	(rad)
β	angle of sideslip the fuselage	(rad)
θ_0	main rotor collective pitch angle	(rad)
$\theta_{1_s}, \theta_{1_c}$	main rotor longitudinal and lateral cyclic pitch angles	(rad)
$\tau_{e_1}, \tau_{e_2}, \tau_{e_3}$	engine and rotorspeed governor time constants	(s)
ϕ, θ, ψ	body roll, pitch and sideslip attitude angles	(rad)
$\dot{\chi}$	turn rate	(rad/s)
Ω	angular velocity of main rotor	(rad/s)
Ω_{idle}	angular velocity of main rotor at idle	(rad/s)
Ω_{TR}	angular velocity of tail rotor	(rad/s)

1. Introduction

The conventional approach to aircraft flight simulation is to use an appropriate mathematical model of a subject vehicle to compute its response to a set of piloting commands [1]. When the equations of motion which constitute the mathematical model are solved in real-time, and the computed response is used to drive a motion and/or visual system, the simulation may be used for training and vehicle evaluation. This is of course the most widely understood application of flight simulation. Also of interest is the situation where a more comprehensive model (not normally implemented in real-time) is used to investigate detailed aerodynamic or loading situations in the extremities of the flight envelope. Simplified linearised models may also be used to establish the stability characteristics of aircraft. One of the most challenging aerospace applications of simulation is when the vehicle of interest is a rotorcraft. Here as well as modelling the characteristics of the fuselage, the aerodynamic and elastic properties of the rotor blades must also be represented [2, 3].

The alternative approach of *inverse simulation* has recently found wider application in the aerospace field [4, 5]. In the aerospace context an inverse simulation is used to obtain a unique set of control responses which enable the modelled vehicle to traverse a given flight path. There are certain problems in fixed wing flight mechanics where inverse simulate has distinct advantages, the study of manoeuvres at high angle of attack, for example. The main aim of this paper, however, is to show the wide range of problems in the field of rotary-wing flight mechanics to which inverse simulation may applied [6, 7, 8]. Inverse simulation is particularly suited here due to the flight path oriented nature of many helicopter tasks. Examples of such tasks might include take-off and landing in confined spaces, and military helicopters performing nap-of-the-earth flight. The influence of the manoeuvre on helicopter performance has been recognised by the authors of the current U.S. Military Handling Qualities Requirements [9]. Compliance with these requirements is achieved only by demonstrating adequate handling qualities whilst performing specified manoeuvres or Mission Task Elements.

Where a particular flight mechanics problem is associated with a single manoeuvre or series of manoeuvres it is possible, as will become apparent, to create mathematical descriptions of the flight paths and use them to drive an inverse simulation. Both the vehicle's response (in terms of its state vector) and also the control displacements that a modelled helicopter would require to fly it will be obtained. This information may then be used to analyse both the performance of the helicopter, and the required control strategy.

Work in the inverse simulation of helicopters has been progressing at Glasgow for several years, mainly through the development of the package, Helinv [10], and the aim of this report is to give a definitive statement on the numerical algorithm used. The current version (v6) is significantly different from the previously reported version (v2), [10] and it is hoped that this document will give a comprehensive insight into its structure. A detailed description of the algorithm is given in the following section. This is followed by a verification of the algorithm and a validation of the model. Some of the implications of using this type of algorithm are then discussed, and the report is completed by a description of an alternative algorithm.

2. The Helinv Inverse Simulation Algorithm

The simulation exercise of calculating a system's response to a particular sequence of control inputs is well known. It is conveniently expressed as the initial value problem:

$$\dot{\underset{\sim}{x}} = f(\underset{\sim}{x}, \underset{\sim}{u}); \quad \underset{\sim}{x}(0) = \underset{\sim}{x}_0 \tag{1}$$

$$\underset{\sim}{y} = g(\underset{\sim}{x}) \tag{2}$$

where $\underset{\sim}{x}$ is the state vector of the system and $\underset{\sim}{u}$ is the control vector. Equation (1) is a statement of the mathematical model which describes the time-evolution of the state vector in response to an imposed time history for the control vector $\underset{\sim}{u}$. The output equation, (2), is a statement of how the observed output vector $\underset{\sim}{y}$ is obtained from the state vector.

Inverse simulation is so called because, from a pre-determined output vector $\underset{\sim}{y}$ it calculates the control time-histories required to produce $\underset{\sim}{y}$. Consequently, equations (1) and (2) are used in an implicit manner and, just as conventional simulation attaches importance to careful selection of the input $\underset{\sim}{u}$, inverse simulation places emphasis on the careful definition of the required output $\underset{\sim}{y}$. Before detailing the inverse method inherent in Helinv it is necessary to first discuss the mathematical model it uses, HGS (Helicopter Generic Simulation) [11].

2.1 Helicopter Generic Simulation

For the purpose of this paper only the most elemental version of the model will be discussed (i.e. only the fuselage and rotorspeed degrees of freedom are incorporated) so that the state vector is

$$\underset{\sim}{x} = [u\ v\ w\ p\ q\ r\ \phi\ \theta\ \psi\ \Omega\ Q_E]^T$$

where
- u, v, w are the components of translational velocity relative to a body fixed reference frame (x_b, y_b, z_b),
- p, q, r are angular velocities about the body axes,
- ϕ, θ, ψ are the Euler (or attitude) angles relating the body fixed axes set to the earth fixed inertial frame (x_e, y_e, z_e),
- Ω is the angular velocity of the main rotor and
- Q_E is the torque output of the engines.

Other more comprehensive models include the rotor blade flapping and lagging as states (individual blades have *lagging* motion in the plane of the "disc" to alleviate the hub moment due to aerodynamic drag and *flapping* motion out of the disc plane due to aerodynamic lift) and the dynamics of the rotor induced flow are also often included. In the version of the HGS model referred to in this document these effects are assumed to occur instantaneously and the values of the states associated with these motions are obtained via intermediate calculations.

The control vector may be written as

$$\underset{\sim}{u} = [\theta_0 \; \theta_{1_s} \; \theta_{1_c} \; \theta_{0_{tr}}]^T$$

where θ_0, θ_{1_s}, θ_{1_c}, and $\theta_{0_{tr}}$ represent main and tail rotor blade pitch angles. It is appropriate at this point to discuss briefly the method of control of a conventional helicopter. The basic control method is by varying the magnitude and direction of the main rotor thrust vector. The magnitude of the thrust is controlled by collectively altering the pitch (and hence lift) of all of the rotor blades together by an means of the *collective lever*, θ_0. As well as collective pitch control the pilot is also able to vary the pitch of individual blades cyclically around a complete revolution. When the pilot applies *longitudinal cyclic*, θ_{1_s}, by pushing the *cyclic stick* forward, the blade travelling towards rear of the disc flaps upwards out of the disc plane, whilst the blade travelling towards the front of the disc flaps downwards. The net effect is that the thrust vector is tilted forward allowing accelerated flight in this direction. Similarly pushing the cyclic stick to one side (i.e. applying *lateral cyclic* pitch, θ_{1_c}) increases the pitch of the blades on the opposite side of the rotor (producing upwards flap) and decreasing it on the other (producing downwards flap) thereby producing a net thrust tilt in the direction of the stick motion. This can be used to produce sideways or banked flight. Finally, the torque transmitted by the engine to the main rotor is balanced by an opposing moment produced due to the offset of the tailrotor thrust from the centre of gravity. The tailrotor thrust is controlled through pedal displacements which alter the pitch of the blades, $\theta_{0_{tr}}$, and by varying this thrust (and hence "anti-torque" moment) it is possible to control the heading of the aircraft.

The coupling problems associated with helicopter control can be appreciated by considering the simple example of a pilot wishing to accelerate his aircraft without changing heading or altitude. The acceleration is achieved by application of forward cyclic, θ_{1_s}, which tilts the rotor disc forward. One effect of this is that the component of the thrust vector which balances the weight of the aircraft has been reduced, and hence if altitude is to be maintained the magnitude of the thrust vector must be increased by application of collective pitch, θ_0.

The increased pitch causes increased blade drag and in order to maintain rotorspeed, engine torque is also increased and hence a tailrotor collective pitch, $\theta_{0_{tr}}$, input is required to maintain heading. If unopposed the change in sideforce due to the change in tailrotor thrust will cause the helicopter to drift to the side. To overcome this an opposing input in lateral cyclic is required, θ_{1_c}. Of course the pilot's workload is kept at acceptable levels by introducing control mixing (via mechanical linkages or the Automatic Flight Control System), and equipping the helicopter with a rotorspeed governor, however this simple example, where inputs to all four control channels are required to undertake a very basic manoeuvre, does demonstrate the complexity of the system being modelled.

Considering again equation (1), the function f consists, essentially, of the following equations. The fuselage degrees of freedom are captured by the familiar Euler rigid body equations :

$$\dot{u} = -(w\,q - v\,r) + \frac{X}{m} - g\sin\theta \tag{4.1}$$

$$\dot{v} = -(u\,r - w\,p) + \frac{Y}{m} + g\cos\theta\sin\phi \tag{4.2}$$

$$\dot{w} = -(v\,p - u\,q) + \frac{Z}{m} + g\cos\theta\cos\phi \tag{4.3}$$

$$I_{xx}\,\dot{p} = (I_{yy} - I_{zz})\,q\,r + I_{xz}\,(\dot{r} + p\,q) + L \tag{4.4}$$

$$I_{yy}\,\dot{q} = (I_{zz} - I_{xx})\,r\,p + I_{xz}\,(r^2 - p^2) + M \tag{4.5}$$

$$I_{zz}\,\dot{r} = (I_{xx} - I_{yy})\,p\,q + I_{xz}\,(\dot{p} - q\,r) + N \tag{4.6}$$

where m, I_{xx}, I_{yy}, I_{zz}, and I_{xz} are the aircraft's mass, moments of inertia and product of inertia respectively. The symbols used for the vehicle states have their usual meaning as indicated in Figure 1.

The rate of change of the attitude angles are related to the body axes angular velocities by the kinematic expressions

$$\dot{\phi} = p + q\sin\phi\tan\theta + r\cos\phi\tan\theta \tag{4.7}$$

$$\dot{\theta} = q\cos\phi - r\sin\phi \tag{4.8}$$

$$\dot{\psi} = q\sin\phi\sec\theta + r\cos\phi\sec\theta \tag{4.9}$$

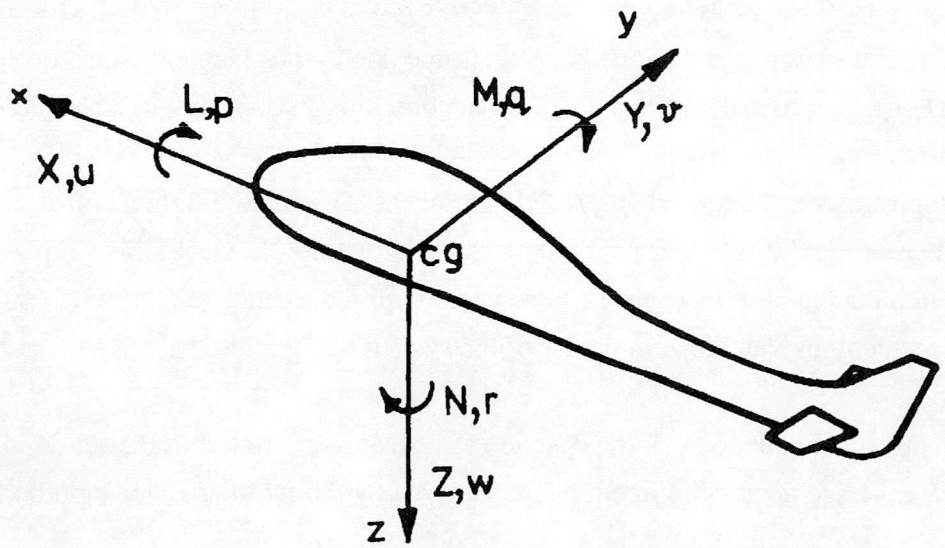

Figure 1 : The Body Fixed Reference Frame

where ψ is the fuselage heading or azimuth angle. Finally, the rotorspeed governor equations as given by Padfield [12] are

$$\ddot{Q}_E = \frac{1}{\tau_{e_1}\tau_{e_2}} \left[- (\tau_{e_1} + \tau_{e_3})\dot{Q}_E - Q_E + K_3 (\Omega - \Omega_{idle} + \tau_{e_2} \dot{\Omega}) \right] \tag{4.10}$$

$$\dot{\Omega} = (Q_E - Q_R - Q_{TR} - Q_{tr})/I_R + \dot{r} \tag{4.11}$$

where	$\tau_{e_1}, \tau_{e_2}, \tau_{e_3}, K_3$	are the time constants and gain of the governor,
	Ω_{idle}	is the angular velocity of the rotor in idle,
	Q_R, Q_{TR}, Q_{tr}	are the torques required to drive the main rotor, tailrotor and transmission, and
	I_R	is the effective inertia of the rotor system.

Equations (4.1 - 4.9) are of course not unique to the helicopter, they are widely used in many rigid body simulations, and it is in the calculation of the external forces and moments X, Y, Z, L, M, N that the modelling effort is required. To derive expressions for the external force and moments individual components of the vehicle are considered - the fuselage (including fin and tailplane), the main rotor and the tail rotor. The external forces and moments on the fuselage are entirely due to the aerodynamic loading and are calculated from look-up tables of appropriate wind tunnel data. In the context of flight simulation this is generally accepted as the most effective solution as computational aerodynamic techniques

tend to be "processor intensive" particularly for the complex flow field and fuselage shape of a helicopter. The look-up tables give force and moment coefficients as functions of the incidence angles α (angle of attack) and β (angle of sideslip) which are given by

$$\tan\alpha = \frac{w}{u} \quad \text{and} \quad \sin\beta = \frac{v}{V_f} \tag{5}$$

where $V_f = \sqrt{u^2 + v^2 + w^2}$ = the flight velocity of the aircraft, and are therefore functions of the state vector.

The external forces and moments from the main rotor are calculated by obtaining expressions for the aerodynamic loads on a blade element, then summing these along the span of the blade, and around a complete revolution of the its travel. The lift and drag of each element will be a function of :

i) the local airstream velocity - this is obtained from consideration of the velocity of the centre of gravity (u, v, w), the angular velocity of the aircraft (p, q, r), the position of the element relative to the c.g. (dependant on hub location, spanwise position and azimuthal location of blade), and the angular velocity of the blade element relative to the body fixed frame (a function of the angular velocity of the rotor Ω as well as the flapping velocity $\dot{\beta}$),

ii) the local angle of attack - as well as being dependant the local velocity, this is a function of the blade control angles θ_0 (constant for the full rotation), θ_{1_s} and θ_{1_c} (dependant on azimuthal position of blade), and the blade twist. (This is a function of radial position - rotor blades are usually twisted with leading edge down towards the tip of the blade where the highest velocities are experienced. This is to ensure more even distribution of the aerodynamic lift along the span thereby reducing the structural bending moment at the root).

For the HGS model this summation has been performed symbolically to produce a series of complex expressions for the external loads of the complete rotor disc which are, as is apparent from above, nonlinear functions of all of the state and control variables. A more sophisticated approach involves performing the summations numerically for each blade. This so called "individual blade model" is of course much more computationally intensive but is now found in wider use [13, 14].

Naturally expressions for the tailrotor external forces and moments are obtained in a similar manner to that described for the main rotor.

2.2 The Helinv Inverse Simulation Technique

Helinv, incorporates several sets of pre-programmed manoeuvre descriptions which are required as system outputs from the simulation. In fact, the manoeuvres are essentially the input into the simulation and much of the value of Helinv lies in the scope and validity of the library of manoeuvre descriptions which have been accumulated. They include those relating to Nap of the Earth [15], Off-shore Operations [8], Mission Task Elements [7], and there is also a facility for accessing flight test data.

The focus of the work at Glasgow is on manoeuvres that are defined in terms of motion relative to an Earth-fixed frame of reference so that the output equation is the transformation of the body-fixed velocity components into Earth axes. The output vector is then

$$\underset{\sim}{u} = [x_e \; y_e \; z_e]^T$$

and the relationship between the output and state vector, g, is simply the Euler transformation between the body axes component velocities (u, v, w) and the earth axes components ($\dot{x}_e$, $\dot{y}_e$, $\dot{z}_e$) via the Euler or attitude angles (ϕ, θ, ψ), Figure 2, given by

$$\begin{bmatrix} u \\ v \\ w \end{bmatrix} = \begin{bmatrix} l_1 & l_2 & l_3 \\ m_1 & m_2 & m_3 \\ n_1 & n_2 & n_3 \end{bmatrix} \begin{bmatrix} \dot{x}_e \\ \dot{y}_e \\ \dot{z}_e \end{bmatrix} \qquad (6)$$

where

$$l_1 = \cos\theta \cos\psi$$
$$l_2 = \cos\theta \sin\psi$$
$$l_3 = -\sin\theta$$
$$m_1 = \sin\phi \sin\theta \cos\psi - \cos\phi \sin\psi$$
$$m_2 = \sin\phi \sin\theta \sin\psi + \cos\phi \cos\psi$$
$$m_3 = \sin\phi \cos\theta$$
$$n_1 = \cos\phi \sin\theta \cos\psi + \cos\phi \sin\psi$$
$$n_2 = \cos\phi \sin\theta \sin\psi - \cos\phi \cos\psi$$
$$n_3 = \cos\phi \cos\theta$$

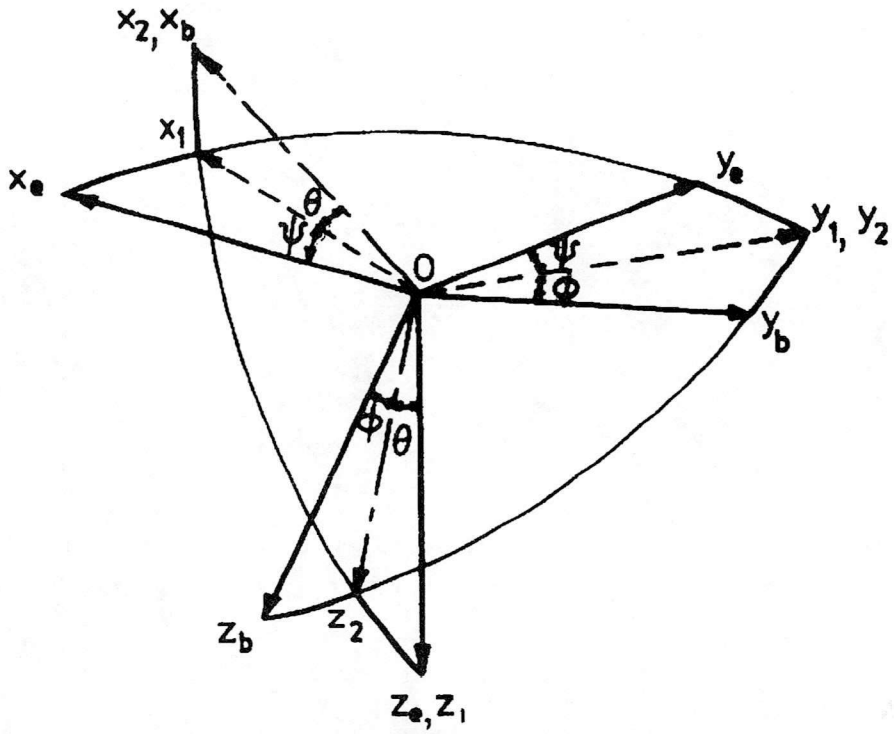

Figure 2 : The Euler Angle Transformation

2.2.1 Definition of Manoeuvres

Manoeuvres are defined by specifying appropriate mathematical functions for the aircraft position as a function of time. For example, the functions

$$z_e(t) = -\left[6\left(\frac{t}{t_m}\right)^5 - 15\left(\frac{t}{t_m}\right)^4 + 10\left(\frac{t}{t_m}\right)^3\right]h$$

$$\dot{y}_e = 0 \qquad (7)$$

describe a "Pop-up" manoeuvre, Figure 3, used to clear some obstacle of height h in a time t_m. A fifth order polynomial is chosen to ensure appropriate levels of derivative continuity and hence smoothness at the start and end of the manoeuvre. The second function ensures that the motion is in the xz plane and that there are no lateral excursions. The x_e co-ordinate may be obtained by further specifying the flight velocity, V_f, as some function of time so that

$$\dot{x}_e(t) = \sqrt{V_f(t)^2 - \dot{z}_e(t)^2 - \dot{y}_e(t)^2} \qquad (8)$$

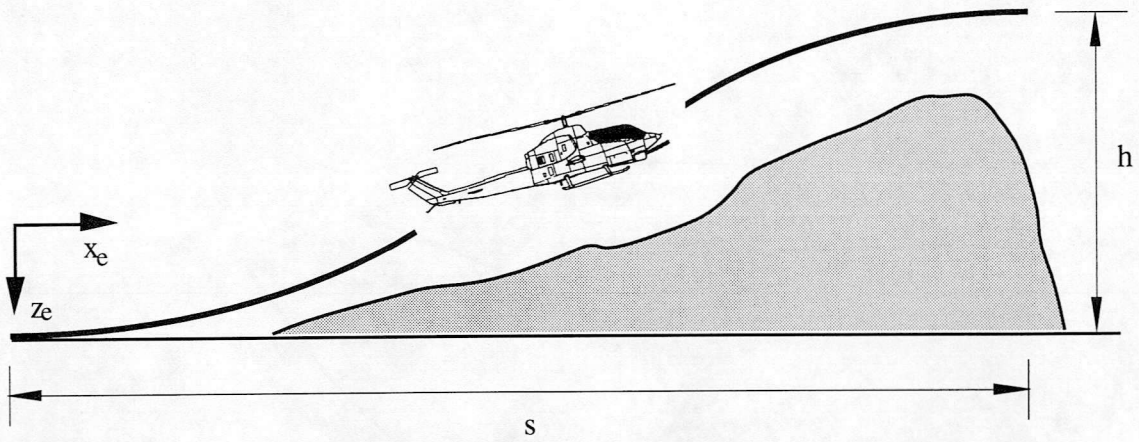

Figure 3 : The Pop-up Manoeuvre

The alternative to direct specification of flight path is to define functions for the vehicle's track angle, $\chi(t)$, and climb angle, $\gamma(t)$, Figure 4, the flight path being obtained from

$$\dot{x}_e(t) = V_f(t)\cos\chi(t)\cos\gamma(t)$$

$$\dot{y}_e(t) = V_f(t)\sin\chi(t)\cos\gamma(t) \qquad (9)$$

$$\dot{z}_e(t) = -V_f(t)\sin\gamma(t)$$

This approach is particularly useful when defining paths for turning flight where the turn rate is specified as a continuous function of time allowing smooth transitions from linear to turning flight and vice versa.

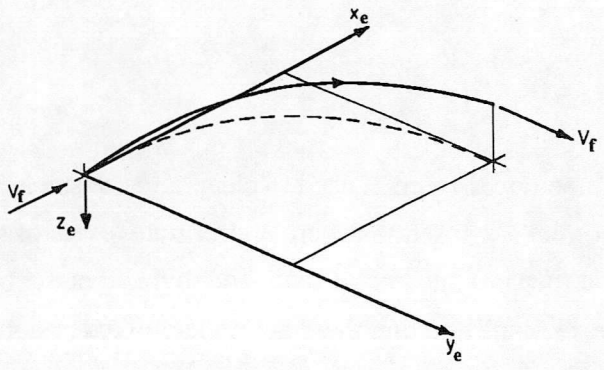

(a) A General 3-Dimensional Manoeuvre

Figure 4 : Definition of a General Manoeuvre

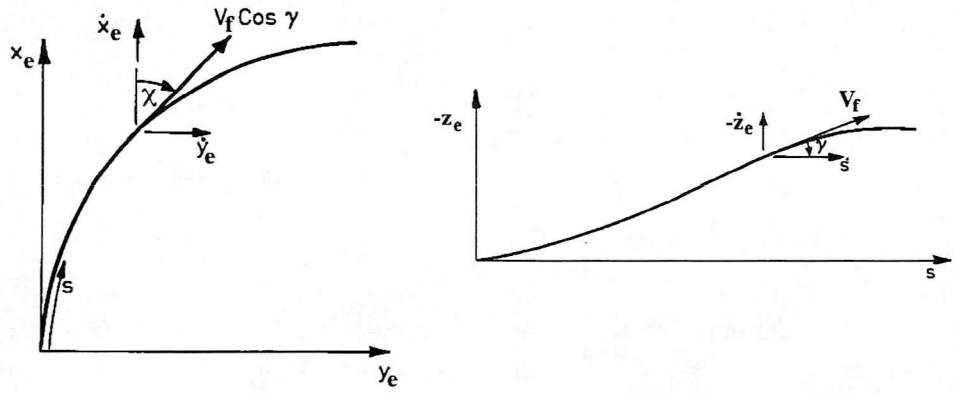

(b) The Track (c) Altitude

Figure 4 : Continued

2.2.2 Constraints

Simply specifying the co-ordinates of the helicopter's c.g. (x_e, y_e, z_e) is insufficient to fully define a manoeuvre a further condition must be applied to fix the orientation of the fuselage relative to the flight path. The choice of which variable to specify (or constrain) is made clearer by considering the influence of the four controls. The main rotor collective will influence the vehicle altitude, z_e, the longitudinal cyclic the fore and aft position, x_e, whilst lateral cyclic will influence the sideways positioning, y_e. This leaves tailrotor collective and the variable most influenced by this control is heading, ψ.

2.2.3 Solving the Equations of Motion

Solving any set of equations one must be clear exactly which variables are known, which are unknown and also which may be found by intermediate calculation, and indeed the order of the intermediate calculations. For the current problem it has been established that the defined variables are the flight path co-ordinates (x_e, y_e, z_e) and aircraft heading, ψ, and that the principle aim is to obtain the unknown control inputs which produce them (θ_0, θ_{1_s}, θ_{1_c}, $\theta_{0_{tr}}$). This is achieved by solution of the six body equations of motion (4.1-4.6) and the engine equation (4.11), with the remaining three unknowns being the fuselage pitch and roll attitudes (θ, ϕ) and the angular velocity of the rotor, Ω. This choice may not at first be clear, however if one considers that when the attitude and earth referenced velocity vector of the vehicle are known it is possible to obtain

i) the body referenced velocity vector (u, v, w) and by differentiation the acceleration vector ($\dot{u}$, $\dot{v}$, $\dot{w}$);

ii) differentiation of the attitudes give the angular velocities (p, q, r) and accelerations ($\dot{p}$, $\dot{q}$, $\dot{r}$);

iii) knowledge of the body velocities will allow the aerodynamic forces on the fuselage to be obtained, whilst the control angles and rotorspeed (and all of the other state information) ensures that the rotor forces may be found, hence the external forces and moments (X, Y, Z, L, M, N) are available.

Examination of the seven equations of motion will show that there is then enough information to obtain values for all of the terms in them, and hence the equations are soluble. This is now discussed in more detail.

The solution is cast in a "time marching" form - that is the input information (the flight path) is expressed as a time series at equally spaced intervals, and the seven equations of motion are solved at each point in the series using the flight path information at that point, and elements of the state vector from the previous time point. If we consider the case of a manoeuvre taking a time t_m, which is divided into a time series of n_{ints} then a general time point in the solution, t_i, may be defined as,

$$0 < t_i \leq t_m \quad \text{where} \quad 1 < i \leq (n_{ints} + 1)$$

The input at this time point is

$$x_{e_i},\ y_{e_i},\ z_{e_i},\ \Psi_i$$

which may be differentiated to give

$$\dot{x}_{e_i},\ \dot{y}_{e_i},\ \dot{z}_{e_i},\ \dot{\Psi}_i \quad \text{and} \quad \ddot{x}_{e_i},\ \ddot{y}_{e_i},\ \ddot{z}_{e_i},\ \ddot{\Psi}_i$$

At each time point values are obtained for all of the unsteady time variant terms in the equations of motion which converts them from differential form to nonlinear, algebraic form. The equations are then solved by a Newton-Raphson iterative technique to find the seven unknowns

$$\theta_i,\ \phi_i,\ \Omega_i,\ \theta_{0_i},\ \theta_{1s_i},\ \theta_{1c_i},\ \theta_{0tr_i}$$

From equations (4.1 - 4.6, and 4.10) the requirement is then to solve:

$$F_1(\theta, \phi, \Omega, \theta_0, \theta_{1s}, \theta_{1c}, \theta_{0tr})_i = \dot{u}_i + (w_i q_i - v_i r_i) - \frac{X_i}{m} + g \sin\theta_i = 0$$

$$\vdots$$

$$F_6(\theta, \phi, \Omega, \theta_0, \theta_{1s}, \theta_{1c}, \theta_{0tr})_i = I_{zz} \dot{r}_i - (I_{xx} - I_{yy}) p_i q_i - I_{xz} (\dot{p}_i - q_i r_i) - N_i = 0 \qquad (10)$$

$$F_7(\theta, \phi, \Omega, \theta_0, \theta_{1s}, \theta_{1c}, \theta_{0tr})_i = \ddot{Q}_{Ei} \tau_{e_1}\tau_{e_2} + (\tau_{e_1}+\tau_{e_3})\dot{Q}_{Ei} + Q_{Ei} - K_3 (\Omega_i - \Omega_{idle} + \tau_{e_2} \dot{\Omega}_i) = 0$$

Clearly from the preceding description of the mathematical model there are many intermediate calculations required. The sequence of calculations at the j^{th} iteration is as follows.

i) Initial Guess of Unknown Variables

The estimate from the previous iteration is used as the initial guess at the current iteration so that

$$\theta_{i,j} = \theta_{i,j-1}, \quad \phi_{i,j} = \phi_{i,j-1}, \quad \text{etc.} \qquad j > 1$$

For the first iteration the converged values from the previous time point are used:

$$\theta_{i,j} = \theta_{i-1}, \quad \phi_{i,j} = \phi_{i-1}, \quad \text{etc.} \qquad j = 1$$

ii) Calculation of the Body Referenced Translational Velocities

The body axes velocities are obtained from the transformation equation (6). The expression for $u_{i,j}$ is

$$u_{i,j} = \dot{x}_{e_i} \cos\theta_{i,j} \cos\psi_i + \dot{y}_{e_i} \cos\theta_{ij} \sin\psi_i - \dot{z}_{e_i} \sin\theta_{i,j} \qquad (11)$$

and similar expressions are obtained for $v_{i,j}$ and $w_{i,j}$.

iii) Rates of Change of Euler Angles and Rotorspeed

Numerical differentiation is used to obtain the Euler angle rates and rate of change of rotorspeed. Backward differencing is used to give the following for $\dot{\theta}_{i,j}$ and $\ddot{\theta}_{i,j}$

$$\dot{\theta}_{i,j} = \frac{\theta_{ij} - \theta_{i-1}}{t_i - t_{i-1}} \qquad \text{and} \qquad \ddot{\theta}_{i,j} = \frac{\theta_{ij} - 2\theta_{i-1} + \theta_{i-2}}{(t_i - t_{i-1})^2} \qquad (12)$$

and similar equations may be obtained for $\dot{\phi}_{ij}$, $\ddot{\phi}_{ij}$, and $\dot{\Omega}_{ij}$. Using numerical differentiation has certain implications on the form of the solution which are discussed in section 4.

iv) Calculation of the Body Referenced Translational Accelerations

The body accelerations are obtained by differentiation of the corresponding velocities, so that for $\dot{u}_{ij}$, from equation (11)

$$\dot{u}_{i,j} = \ddot{x}_{e_i} \cos\theta_{i,j} \cos\psi_i + \ddot{y}_{e_i} \cos\theta_{i,j} \sin\psi_i - \ddot{z}_{e_i} \sin\theta_{i,j} \qquad (13)$$
$$- \dot{\theta}_{i,j} [(\dot{x}_{e_i} \cos\psi_i + \dot{y}_{e_i} \sin\psi_i) \sin\theta_{ij} + \dot{z}_{e_i} \cos\theta_{i,j}] - \dot{\psi}_i [\dot{x}_{e_i} \sin\psi_i - \dot{y}_{e_i} \cos\psi_i]\cos\theta_{i,j}$$

and similar expressions may be obtained for $\dot{v}_{i,j}$ and $\dot{w}_{i,j}$.

v) Calculation of Vehicle Angular Velocities and Accelerations

Equations (4.7 - 4.9) may be recast to give body angular velocities in terms of the Euler angle rates so that, for example, the roll rate, p, may be found from

$$p_{i,j} = \dot{\phi}_{i,j} - \dot{\psi}_i \sin\theta_{i,j} \qquad (14)$$

which may be differentiated to give

$$\dot{p}_{i,j} = \ddot{\phi}_{i,j} - \ddot{\psi}_i \sin\theta_{i,j} - \dot{\psi}_i \dot{\theta}_{i,j} \cos\theta_{i,j} \qquad (15)$$

Expressions for $q_{i,j}$, $r_{i,j}$, $\dot{q}_{i,j}$, and $\dot{r}_{i,j}$ are obtained in a similar way.

vi) The External Forces and Moments

Having established estimates for all of the vehicle states and controls it is possible to evaluate the corresponding external forces and moments : $X_{i,j}$, $Y_{i,j}$, $Z_{i,j}$, $L_{i,j}$, $M_{i,j}$, $N_{i,j}$ as discussed in section 2.1.

vii) Engine Torque and its Rate of Change

The torque required to turn the main rotor, $Q_{R_{i,j}}$, tailrotor, $Q_{TR_{i,j}}$, and transmission, $Q_{tr_{i,j}}$, are obtained from the calculation of external forces and moments. These values are then used in association with equation (4.11) to obtain the required engine torque

$$Q_{Ei,j} = (\dot{\Omega}_{i,j} - \dot{r}_{i,j}) I_R + Q_{Ri,j} + Q_{TRi,j} + Q_{tri,j} \quad (16)$$

The rates of change of engine torque, $\dot{Q}_{Ei,j}$ and $\ddot{Q}_{Ei,j}$, are calculated by numerical differentiation using the values of engine torque from the previous two time points (Q_{Ei-1}, Q_{Ei-2}) in the same was as shown in equation (12).

It is now possible to obtain the values for the seven functions at the j^{th} iteration. If the solution has not converged (i.e. if the functions have not reached within a small tolerance of zero) then new estimates of the unknown variables are found. The new estimates are found from

$$\begin{bmatrix} \theta_{i,j+1} \\ \vdots \\ \vdots \\ \theta_{0tr_{i,j+1}} \end{bmatrix} = \begin{bmatrix} \theta_{i,j} \\ \vdots \\ \vdots \\ \theta_{0tr_{i,j}} \end{bmatrix} - \begin{bmatrix} \left(\frac{\partial F_1}{\partial \theta}\right)_{i,j} & \cdots & \cdots & \left(\frac{\partial F_1}{\partial \theta_{0tr}}\right)_{i,j} \\ \vdots & & & \vdots \\ \vdots & & & \vdots \\ \left(\frac{\partial F_7}{\partial \theta}\right)_{i,j} & \cdots & \cdots & \left(\frac{\partial F_7}{\partial \theta_{0tr}}\right)_{i,j} \end{bmatrix}^{-1} \begin{bmatrix} F_1(\theta,\phi,\Omega,\theta_0,\theta_{1s},\theta_{1c},\theta_{0tr})_{i,j} \\ \vdots \\ \vdots \\ F_7(\theta,\phi,\Omega,\theta_0,\theta_{1s},\theta_{1c},\theta_{0tr})_{i,j} \end{bmatrix} \quad (17)$$

The Jacobian elements are calculated by numerical differentiation, so that, for example

$$\left(\frac{\partial F_1}{\partial \theta}\right)_{i,j} = \frac{F_1(\theta+\delta\theta,\phi,\ldots,\theta_{0tr})_{i,j} - F_1(\theta-\delta\theta,\phi,\ldots,\theta_{0tr})_{i,j}}{2\delta\theta} \quad (18)$$

for a small perturbation in θ, $\delta\theta$.

It is clear then that all seven functions must be calculated at positive and negative perturbations from their current estimates and hence steps (ii) - (vii) must be performed a further fourteen times.

With new estimates calculated the iteration continues in a conventional way.

2.3 Example of Helicopter Inverse Simulation

The mathematical model described above has been implemented in a generic form such that any helicopter of the single main and tail rotor class can be simulated by specifying an appropriate set of configurational data. This is demonstrated by the following example of inverse simulations of two different helicopters: the Westland Lynx and Aerospatiale (Eurocopter) Puma flying an identical manoeuvre. The configurational data is as given by Padfield [12] whilst the manoeuvre is a Pop-up (as described above) performed at a constant

velocity (V_f) of 80 knots, to clear an obstacle of height (h) of 25m, whilst the manoeuvre time (t_m) is calculated to give a distance covered of 200m. Results for inverse simulations of the two configurations flying this manoeuvre are presented in Figure 5 below.

Although both aircraft have basically the same configuration (single, 4 bladed main rotors etc), the basic design on the rotors are significantly different thereby imparting different characteristics. The Lynx, in fact, has what is termed a "semi-rigid" rotor as it does not possess flapping hinges (the moment produced at the root being reacted by the structural stiffness of flexible titanium alloy sections) whilst the Puma has a "fully articulated" (i.e. hinged) rotor. This gives the Lynx greater agility with faster rate response to control inputs and ultimately smaller cyclic control inputs to achieve a particular attitude displacement. This is evident from the plot of longitudinal cyclic (which produces the pitching moment and hence pitch attitude) where the displacements required by the Lynx are much smaller than those of the Puma. Note that as both aircraft are flying the same manoeuvre the kinematics of the task are the same and therefore so is the pitch attitude. The roll attitude and tailrotor collective are in the opposite sense to one another as the rotors rotate in opposite directions. The Puma is also a larger aircraft with a greater disc loading than the Lynx and so larger collective inputs are also required.

This example demonstrates one of the main advantages in using inverse simulation: having defined the operational task (or more likely a series of tasks as with the ADS 33C handling qualities requirements [9]) it is possible to simulate several vehicles or several variants of the same vehicle performing this task. As well as the results shown in Figure 5, it is also possible to obtain the power and torque required as well as many other parameters providing useful performance information.

2.4 Verification and Validation of the Helinv Algorithm

It is a fairly simple matter to qualitatively assess the accuracy of the results from inverse simulation - the control inputs and state responses calculated to fly specific manoeuvres can be usually be explained in a convincing manner in the context of the likely response of the real aircraft. Of course a more rigorous approach is required and in common with other simulations this is treated in two parts. Firstly it is important to verify that the algorithm is functioning correctly. This is achieved by applying the control inputs derived from the inverse simulation to the corresponding conventional simulation. In verifying the Helinv algorithm this is a simple process as the inherent model, HGS is also available in the

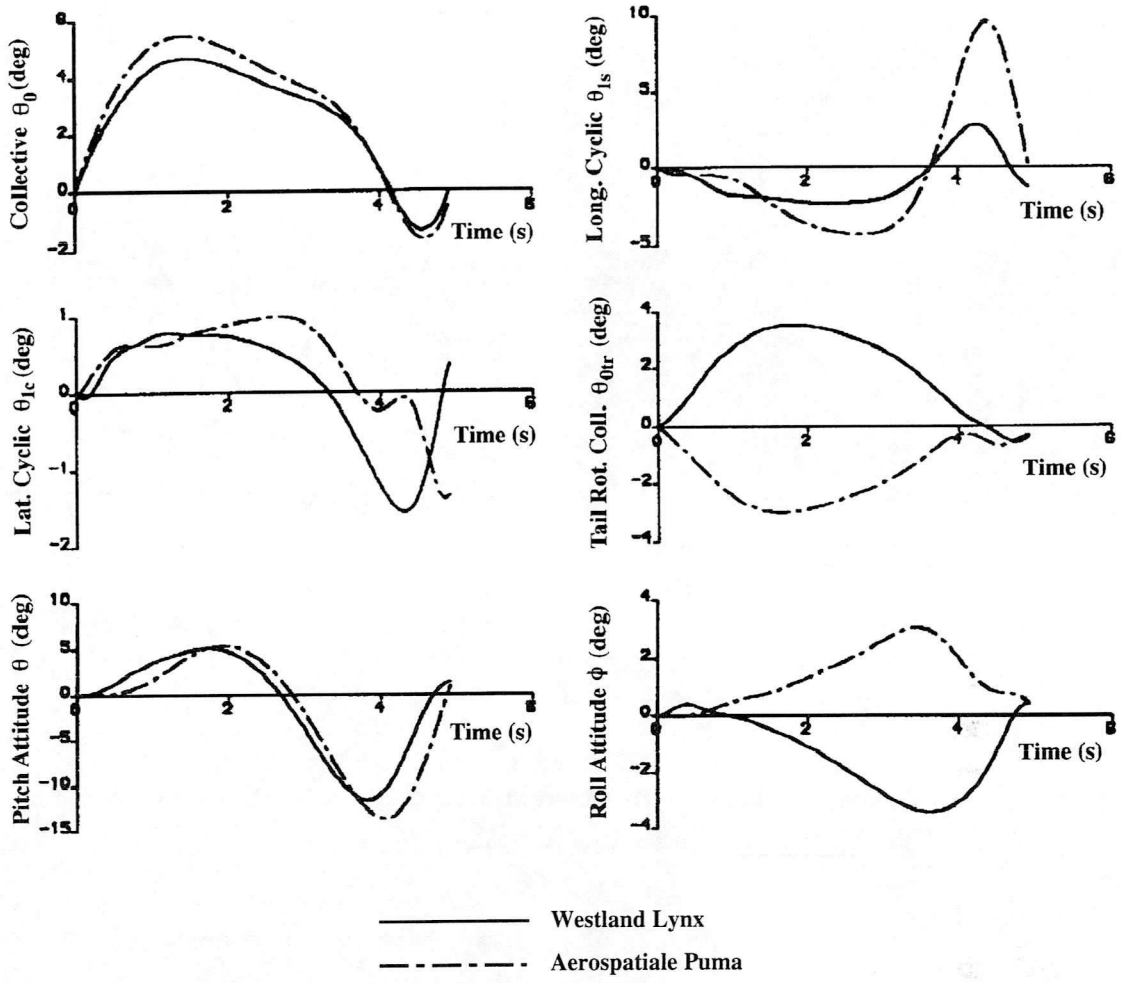

Figure 5 : Inverse Simulation Results for 2 Configurations Flying a Pop-up Manoeuvre

form of a conventional flight mechanics simulation. The verification process then consists of obtaining the control time histories required to fly a predetermined flight path, use these to drive the conventional simulation calculating the flight path that they produce, then comparing this with the path used to drive the inverse simulation. Clearly, if the inverse simulation is functioning correctly then the control inputs should produce the same flight path (irrespective of whether the helicopter model is valid or not). An example of this is shown in Figure 6 where the control inputs for the Lynx shown in Figure 4 have been applied to the HGS model to derive the flight path response. The two flight paths are shown in Figure 6. From the plot of altitude it is obvious that there is little difference between the two (only a very slight deviation at the end of the manoeuvre). The plot of the track should be a straight line along the x-axis shows a deviation of less than 5cm over the 200m distance. These and similar results provide sufficient evidence that the algorithm is functioning in the intended manner.

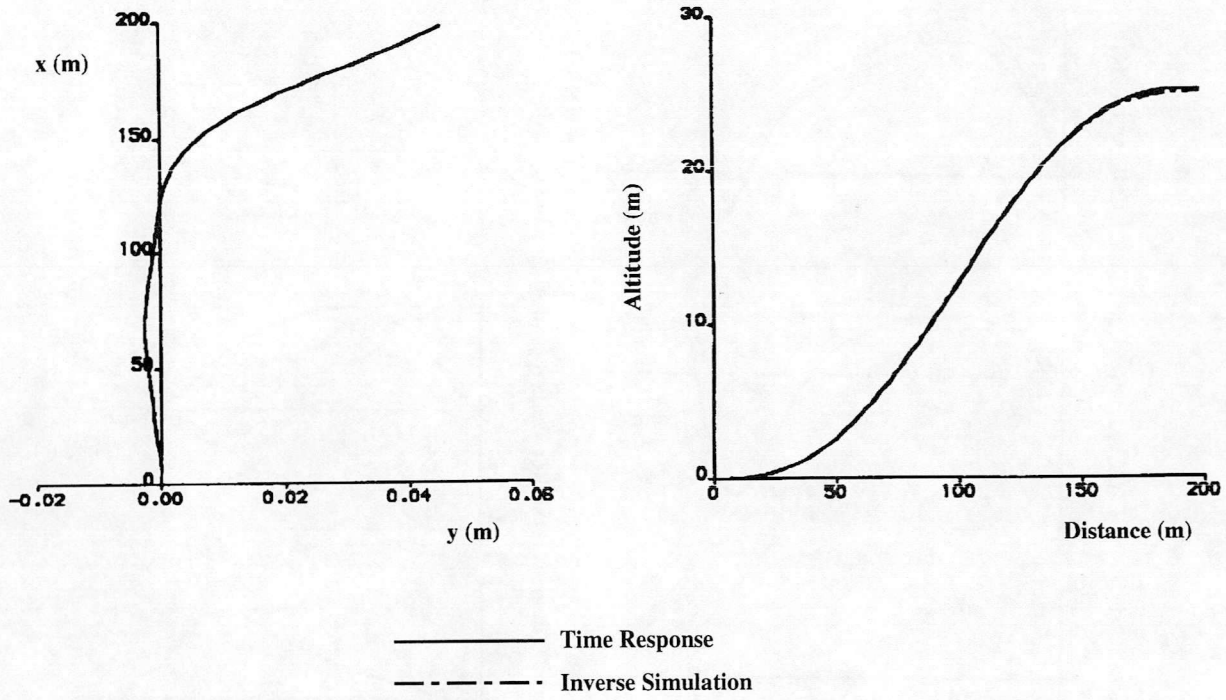

Figure 6 : Comparison of Flight Paths - Original Defined Path vs Path Generated by Time Response Driven by Calculated Controls

The question of the validity of the results is also important - if any meaningful information is to be derived then the mathematical model must replicate the actions of the real aircraft. Inverse simulation provides a useful technique for validating mathematical models. The conventional approach is to apply identical inputs to both the model and the system being simulated and then compare the two responses. Inverse simulation allows the actual system response to be used as an input to the model, the aim being to predict the control actions that were required to produce it. The actual and predicted control inputs may then be compared and the validity of the model established. It should be noted that all of the state responses are also calculated and are comparable with the actual system data. The main advantages of this approach are discussed in Reference 16.

An example of such a validation exercise is demonstrated in Figure 7. Data from flight trials of a Westland Lynx helicopter were supplied by the Defence Research Agency [7] which included time histories of all of the states and controls as well as ground based measurements of the helicopter's position. The positional co-ordinates and heading histories were used as inputs to Helinv, whilst the response histories are compared with those calculated by Helinv. The manoeuvre featured in Figure 7 is a "Quick-hop" which is a rapid longitudinal translation at constant height and heading, from a hover flight state over a

specified distance (in this example 300ft) ending in a stabilised hover. The comparison between flight data and simulation shows that the correct trend is being predicted in all

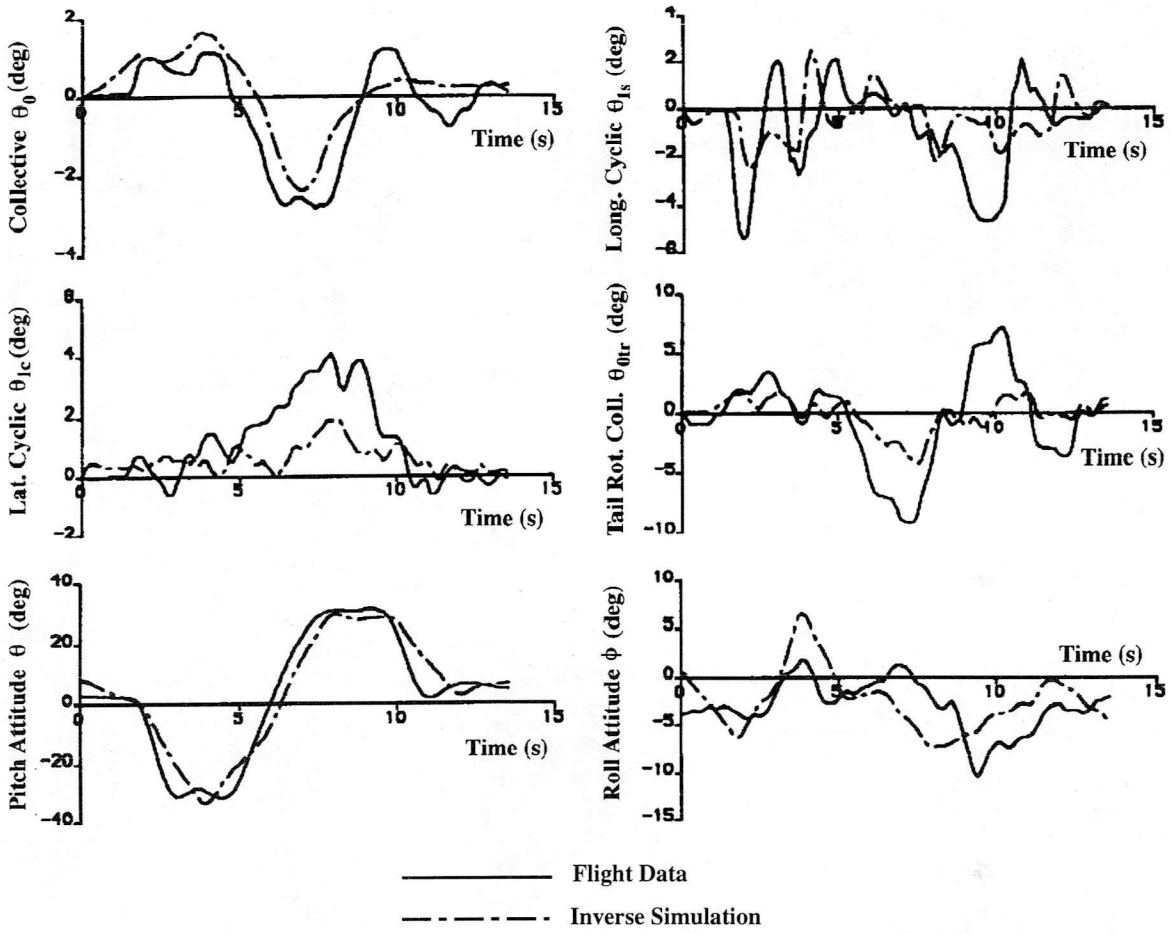

Figure 6 : Comparison of Flight Data and Inverse Simulation Results for a "Quick-hop" Manoeuvre

controls albeit with different absolute displacements in some variables (lateral cyclic and tail rotor for example). Other variable show good prediction qualitative and quantitative agreement - pitch attitude and collective for example. These and other results suggest that the model is of sufficient fidelity to be a useful tool for flight mechanics studies.

3. The Effect of Constraining the Motion of the Helicopter

There is a marked difference between the responses calculated using inverse simulation and those from a conventional simulation. Solving the initial value problem for the state response due to a certain input gives effectively the open loop free response of the aircraft. This contrasts with the inverse simulation where the translational motion and heading of the aircraft are constrained by the defining function of the trajectory. In effect the aircraft has been given a control system with infinite feedback on position and heading and it is then natural that the aircraft's dynamic characteristics will be quite different from those of the unconstrained aircraft. This effect can be quantified by using a linearised model of the helicopter [18] which can be expressed in the standard state space form :

$$\dot{\underset{\sim}{x}} = \mathbf{A}\,\underset{\sim}{x} + \mathbf{B}\,\underset{\sim}{u} \tag{19}$$

where $\underset{\sim}{x}$ and $\underset{\sim}{u}$ are the state and control vectors (as given in section 2.1), **A**, the system matrix and **B** the control matrix. The state vector can be split into sub-vectors: $\underset{\sim}{x}_1$, consisting of the states strongly influenced by the applied constraints, and $\underset{\sim}{x}_2$ consisting of the other unconstrained states. The applied constraints are the three positional co-ordinates (x_e, y_e, z_e) and heading, ψ forming the vector, $\underset{\sim}{f}_c$, and the states most influenced by them are u, v, w, and r. This gives

$$\underset{\sim}{x}_1 = \begin{bmatrix} u \\ v \\ w \\ r \end{bmatrix}, \qquad \underset{\sim}{x}_2 = \begin{bmatrix} p \\ q \\ \phi \\ \theta \end{bmatrix}, \qquad \underset{\sim}{f}_c = \begin{bmatrix} x_e \\ y_e \\ z_e \\ \psi \end{bmatrix}$$

The aim is to produce a state space representation (in the same form as equation (19)) of the inverse problem. The input vector in the inverse simulation will be the constraints, $\underset{\sim}{f}_c$, whilst the output vector will be the unconstrained states, $\underset{\sim}{x}_2$.

The system can then be partitioned to give:

$$\begin{bmatrix} \dot{\underset{\sim}{x}}_1 \\ \dot{\underset{\sim}{x}}_2 \end{bmatrix} = \left[\begin{array}{c|c} \mathbf{A_{11}} & \mathbf{A_{12}} \\ \hline \mathbf{A_{21}} & \mathbf{A_{22}} \end{array}\right] \begin{bmatrix} \underset{\sim}{x}_1 \\ \underset{\sim}{x}_2 \end{bmatrix} + \begin{bmatrix} \mathbf{B_1} \\ \hline \mathbf{B_2} \end{bmatrix} \begin{bmatrix} u \\ \sim \end{bmatrix} \tag{20}$$

which can be expanded to give two linear differential equations:

$$\dot{\underset{\sim}{x}}_1 = \mathbf{A_{11}}\,\underset{\sim}{x}_1 + \mathbf{A_{12}}\,\underset{\sim}{x}_1 + \mathbf{B_1}\,\underset{\sim}{u} \tag{21}$$

$$\dot{\underset{\sim}{x}}_2 = \mathbf{A_{21}}\,\underset{\sim}{x}_1 + \mathbf{A_{22}}\,\underset{\sim}{x}_1 + \mathbf{B_2}\,\underset{\sim}{u} \tag{22}$$

and the control vector can be eliminated from equations (21) and (22) giving

$$\dot{\underset{\sim}{x}}_2 = \left[\mathbf{A_{22}} - \left(\mathbf{B_2 B_1^{-1}}\right)\mathbf{A_{12}}\right]\underset{\sim}{x}_2 + \left[\left(\mathbf{A_{21}} - \left(\mathbf{B_2 B_1^{-1}}\right)\mathbf{A_{11}}\right)\underset{\sim}{x}_1 - \left(\mathbf{B_2 B_1^{-1}}\right)\dot{\underset{\sim}{x}}_1\right] \tag{23}$$

The vector of strongly influenced states, $\underset{\sim}{x}_1$ can be expressed in terms of the vector of applied constraints [18], $\underset{\sim}{f}_c$ and equation (23) can then be written in the form

$$\dot{\underset{\sim}{x}}_2 = \mathbf{A_c}\,\underset{\sim}{x}_2 + \mathbf{B_c}\,\underset{\sim}{u}_c \tag{24}$$

where $\underset{\sim}{u}_c = [\underset{\sim}{f}_c \;\; \dot{\underset{\sim}{f}}_c \;\; \ddot{\underset{\sim}{f}}_c]^T$.

Equation (24) then expresses the inverse problem in state space form and the dynamic characteristics of the helicopter in constrained flight will come not form the "free" system matrix **A**, but from the "constrained" system matrix $\mathbf{A_c}$.

The effect of constraining the helicopter to fly a precise path can be quantified by using appropriate numerical values for the system and control matrices **A**, and **B**. The submatrices ($\mathbf{A_{11}}$, $\mathbf{A_{12}}$ etc) may then be formed, and the constrained system matrix $\mathbf{A_c}$ calculated. Such an exercise has been performed [18] using data for the Westland Lynx at low speed. The dynamic characteristics are of course given by the eigenvalues of the respective system matrices, and in the case of the constrained system lightly damped oscillatory modes with periods of around 1 second are found. The unconstrained system eigenvalues on the other hand predict oscillatory modes with periods of several seconds over a similar speed range.

This predicted effect is often visible on data recorded during flight trials involving manoeuvres where tightly defined manoeuvres are performed. Further, the nonlinear inverse simulation, Helinv, also exhibits these moderately high frequency oscillations superimposed over the main response. This is discussed more fully in the following section.

4. The Implications of Using Numerical Differentiation in an Inverse Simulation Algorithm

It was shown in section 2 that as part of the discretisation process used to solve the equations of motion, numerical differentiation is used to obtain values for the rates of change of θ, ϕ and Ω. The real advantage of this approach is that the resulting algorithm is relatively economical in computational time, however there are some drawbacks. The main one is that in common with any other scheme using numerical differencing it is prone to rounding errors when subtracting similar numbers. There are two possible situations where this may arise: attempting to differentiate a slowly changing variable using a small time increment, and in calculating the Jacobian where the functions to be differentiated may not be sensitive to small increments of the unknown variables. Careful selection of both the time increment used in the discretisation, and the increments used for the Jacobian calculation are therefore essential for a numerically stable solution.

Numerical differentiation also causes problems when modifying the algorithm to include new vehicle states. Apart from requiring some structural modification of the algorithm itself, characteristic frequencies associated with the new modes must also be taken into account. Take for example the inclusion of blade flapping dynamics. The frequency of the motion might typically be around 5 Hz, and therefore in order to capture the effects of the blade flapping, a small time increment will be required. The rigid body modes are much slower (possibly with frequencies of around 0.1 Hz) and consequently there may be numerical problems associated with the rounding errors caused when differencing body states over such a small time increment.

The choice of time increment can also affect the degree to which the constraint influenced oscillations (discussed in the previous section) are visible in the results. The use of larger increments has the effect of damping the oscillations to the extent that they are not visible on the calculated responses. In effect insufficient points are available over the period of the oscillation to fully define it. The oscillations are much more visible when small time increments are used, as shown in the following example. Figure 8 shows two inverse simulation results for a Lynx helicopter flying a Quick-hop manoeuvre. In this case the aircraft accelerates from the hover to a maximum velocity of 40 knots whilst maintaining constant altitude and heading, followed by a deceleration back to the hover. The two results show the effect of reducing the time increment from 0.1 to 0.01 seconds. The appearance of the constraint oscillations superimposed over the main response is evident especially on the time history of longitudinal cyclic.

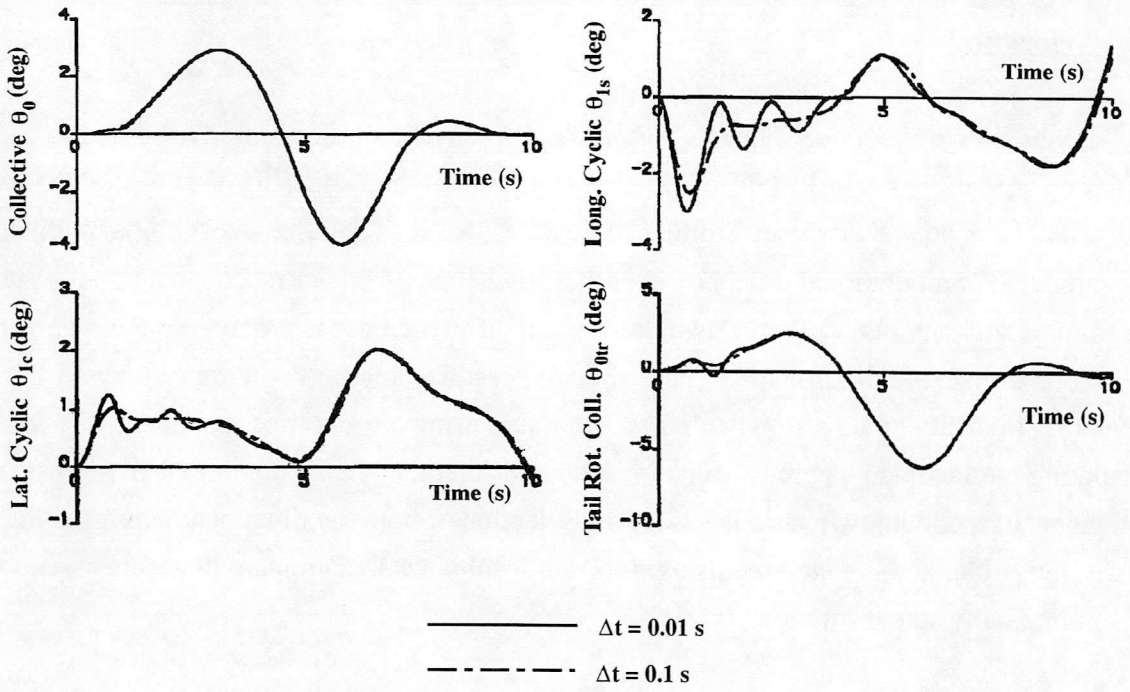

Figure 8 : Inverse Simulation Results for Lynx Flying a Dash-stop Manoeuvre

5. Alternative Inverse Simulation Algorithms

The alternative to using a numerical differentiation process to in an inverse simulation algorithm is to use numerical integration. Consider again that the problem can be discretised over a series of time increments. At a given time point in the solution process where the helicopter has a predefined location and heading, the aim is to calculate the control displacements which will translate the vehicle to the new location and heading at the next time point. If the time increment is small enough it can be assumed that there will exist a set of control step inputs which will achieve this goal. It is then possible to set up an iterative scheme where, firstly, an initial guess of the amplitude of these steps is made. The response of the helicopter over the time increment is then calculated using a numerical integration of the equations of motion, and hence positional and heading change at the new time point are obtained. A new estimate of the amplitude of the steps may then be made based on the error between the calculated and require co-ordinates. This technique is finding wider application [5, 19, 20] as it overcomes many of the problems inherent in the differentiation algorithms. The main drawback is the substantially increased computational time (due to the necessity to repeatedly solve the complete set of equations of motion by numerical integration.

6. Conclusions

The numerical algorithm used in the inverse simulation, Helinv (v6) is described in this paper. From the work presented the following conclusions may be drawn:

1. The Helinv (v6) algorithm produces accurate inverse simulation results for single main and tail rotor helicopters over a wide range of manoeuvres.

2. Although the use of numerical differentiation can produce instability, the algorithm appears to be robust enough to give useful results for a wide range of manoeuvre severity.

3. Schemes using numerical integration as the basis for solving the equations of motion in an inverse manner are more flexible but suffer from being computationally intensive.

4. The high frequency oscillatory modes often present on inverse simulation results are due to the constraints placed on the motion of the aircraft.

References

1. Rolfe, J.M., Staples, K.J., "Flight Simulation", Cambridge University Press, 1989.

2. Bramwell, A.R.S., "Helicopter Dynamics", Arnold, 1976.

3. Prouty, R.W., "Helicopter Performance, Stability and Control", Robert E. Krieger Publishing Company, 1990.

4. Kato, O., Suguira, I., "An Interpretation of Airplane General Motion and Control as Inverse Problem", Journal of Guidance, Control and Dynamics, Vol. 9, No. 2, 1986.

5. Gao, C., Hess, R.A., "Inverse Simulation of Large-Amplitude Aircraft Maneuvers", Journal of Guidance, Control, and Dynamics, Vol. 16, No. 4, 1993.

6. Thomson, D.G., "An Analytical Method of Quantifying Helicopter Agility", Paper 45, Proceedings of the 12th European Rotorcraft Forum, Garmisch-Partenkirchen, Germany, September 1986.

7. Bradley, R., Thomson, D.G., "The Development and Potential of Inverse Simulation for the Quantitative Assessment of Helicopter Handling Qualities", Proceedings of the NASA/AHS Conference 'Piloting Vertical Flight Aircraft: Flying Qualities and Human Factors', San Francisco, January 1993.

8. Thomson, D.G., Talbot, N., Taylor, C., Bradley, R., Ablett, R., "An Investigation of Piloting Strategies for Engine Failures During Take-off from Offshore Platforms", Paper O5, Proceedings of 19th European Rotorcraft Forum, Cernobbio, Italy, September 1993.

9. Anon, "Aeronautical Design Standard, Handling Qualities Requirements for Military Rotorcraft.", ADS-33C, August 1989.

10. Thomson, D.G., Bradley, R., "Development and Verification of an Algorithm for Helicopter Inverse Simulation", Vertica, Vol. 14, No. 2, May 1990.

11. Thomson, D.G., "Development of a Generic Helicopter Model for Application to Inverse Simulation", University of Glasgow, Department of Aerospace Engineering, Internal Report No. 9216, June 1992.

12. Padfield, G.D., "A Theoretical Model of Helicopter Flight Mechanics for Application to Piloted Simulation", Royal Aircraft Establishment, TR 81048, April 1981.

13. McVicar, J.S.G., Bradley, R., "A Generic Tilt-rotor Simulation Model with Parallel Implementation and Partial Periodic Trim Algorithm", Proceedings of the 18th European Rotorcraft Forum, Avignon, France, September 1992.

14. Houston, S.S., "Rotorcraft Simulation for Design Applications", Proceedings of the 1992 European Simulation Multiconference, June 1992.

15. Thomson, D.G., Bradley, R., "Modelling and Classification of Helicopter Combat Manoeuvres", Proceedings of ICAS Congress, Stockholm, Sweden, September 1990.

16. Padfield, G.D., Charlton, M., "Aspects of RAE Flight Research into Helicopter Agility and Pilot Control Strategy", Proceedings of the Specialists Meeting; Aeroflightdynamics Directorate, Ames Research Center, June 1986.

17. Thomson, D.G., Bradley, R., "Prediction of the Dynamic Characteristics of Helicopters in Constrained Flight", The Aeronautical Journal, December 1990.

18. Hess, R.A., Gao, C., "A Generalized Algorithm for Inverse Simulation Applied to Helicopter Maneuvering Flight", Journal of the American Helicopter Society, Vol. 38, No. 4., October 1993

19. Rutherford, S., Thomson, D.G., "A Generalised Inverse Simulation Algorithm", University of Glasgow, Department of Aerospace Engineering